We are IntechOpen, the world's leading publisher of Open Access books
Built by scientists, for scientists

6,900
Open access books available

185,000
International authors and editors

200M
Downloads

154
Countries delivered to

Our authors are among the

TOP 1%
most cited scientists

12.2%
Contributors from top 500 universities

CLARIVATE ANALYTICS
BOOK CITATION INDEX
INDEXED

WEB OF SCIENCE™

Selection of our books indexed in the Book Citation Index
in Web of Science™ Core Collection (BKCI)

Interested in publishing with us?
Contact book.department@intechopen.com

Numbers displayed above are based on latest data collected.
For more information visit www.intechopen.com

Electron Microscopic Recording of Myosin Head Power and Recovery Strokes Using the Gas Environmental Chamber

Haruo Sugi, Tsuyosi Akimoto and Shigeru Chaen

Abstract

Despite extensive studies, the amplitude and the mode of the myosin head movement, coupled with ATP hydrolysis, still remain to be a matter for debate and speculation. To obtain direct information about the ATP-coupled myosin head movement, we prepared synthetic myosin filaments (myosin-myosin rod copolymer), in which myosin heads were position-marked with gold particles via antibodies to myosin heads and kept in hydrated, living state in the gas environmental chamber. ATP was applied to the specimen iontophoretically by passing the current to an ATP-containing microelectrode, and the ATP-induced myosin head movement was recorded with an imaging plate system under a magnification of 10,000×, with the following novel findings: (1) In the absence of ATP, myosin heads fluctuate around a definite neutral position. (2) In the absence of actin filaments, myosin heads move away from the bare region of myosin filaments (recovery stroke, average amplitude, 6 nm) on ATP application and return to the neutral position after exhaustion of ATP. (3) In the presence of actin filaments, the ATP-induced myosin head power stroke exhibits two different modes depending on mechanical conditions. (4) Myosin heads determine the direction of ATP-induced movement without being guided by actin filaments.

Keywords: gas environmental chamber, muscle contraction, myosin head power stroke, myosin head recovery stroke, iontophoretic ATP application

1. Introduction

In 1954, Huxley and Hanson [1] made a monumental discovery that muscle contraction is caused by relative sliding between actin and myosin filaments, which constitute hexagonal lattice structure within muscle fibers. Later, it has been found that (1) a muscle is a machine converting chemical energy derived from ATP hydrolysis into mechanical work and that (2) the sliding between actin and myosin filaments is produced by cyclic attachment-detachment between myosin heads extending from myosin filaments and corresponding myosin-binding sites in actin filaments [2]. **Figure 1** illustrates the most plausible sequence of the actin-myosin interaction in the muscle, producing force and motion in the muscle. In relaxed muscle, individual myosin heads (M) are in the state, M-ADP-Pi, and are detached
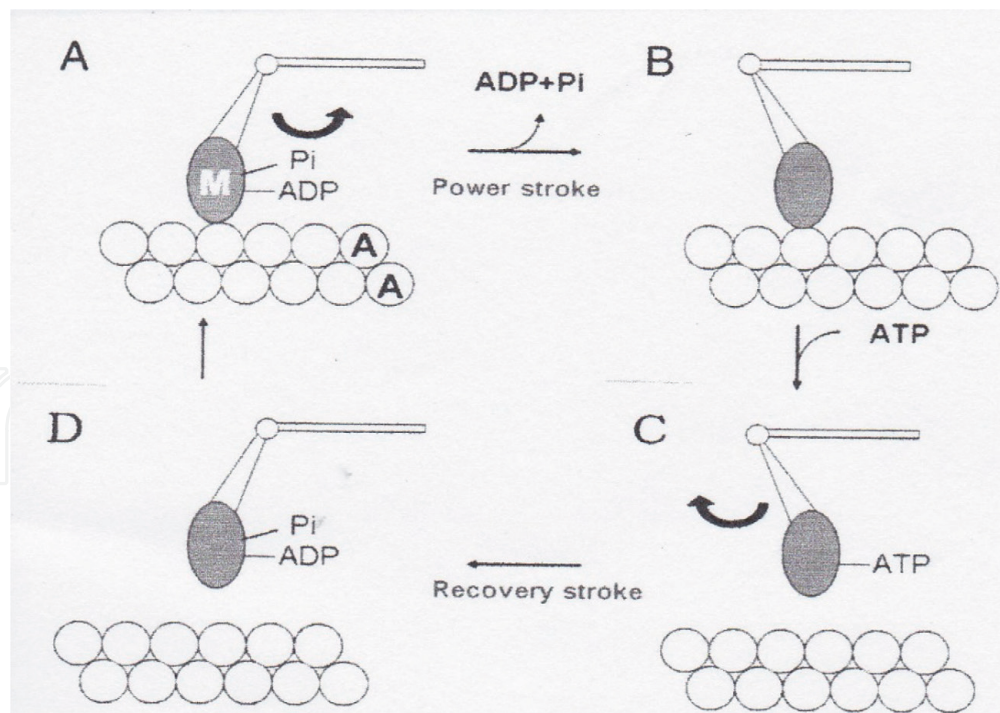
Figure 1.
Schematic diagram showing the most plausible sequence of attachment-detachment cycle between myosin head (M) and actin filament (A), coupled with ATP hydrolysis. From [7].

from actin filaments (A). On stimulation of the muscle, M-ADP-Pi attaches to A and performs a power stroke, associated with the release of Pi and ADP, to produce unitary sliding between actin and myosin filaments (from A to B). After completion of the power stroke, M remains attached to A until the next ATP comes to bind to it (B). On binding with ATP, M detaches from A, and performs a recovery stroke associated with ATP hydrolysis, to form M-ADP-Pi (from C to D). Then, M in the form of M-ADP-Pi again attaches to A to repeat power and recovery strokes.

Despite extensive studies to prove the power and recovery strokes associated with ATP hydrolysis, no definite results have been obtained due to the asynchronous nature of the individual myosin head movement in muscle fibers. In vitro motility assay experiments, in which fluorescently labeled actin filaments are made to slide on myosin molecules or their proteolytic fragments, and optical trap experiments, in which single myosin heads are made to interact with single actin filaments, are not effective in studying myosin head movements in the muscle, since these experiments differ too far from what actually takes place in the myofilament lattice structure constituting the muscle [3].

The most straightforward way to give information about the properties of myosin head power and recovery strokes is to visualize and record myosin head movements associated with ATP hydrolysis, using the gas environmental chamber (EC) attached to an electron microscope. The EC system enables us to insulate biological specimens from high vacuum of the electron microscope and to keep them in wet, living state by constantly circulating water vapor. We started to work with the group of the late Professor Akira Fukami of Nihon University, who developed the EC system together with the Japan Electron Optics Laboratory, Ltd. (JEOL Ltd.) in the late 1980s [4], and after a number of trials and errors, succeeded in obtaining novel results concerning the properties of myosin head power and recovery strokes.

Here, we describe novel properties of myosin heads in producing power and recovery strokes, which can never be obtained by any other experimental methods.

2. The EC system to record ATP-induced myosin head movement

As shown in **Figure 2**, the EC is a cylindrical compartment (inner diameter, 2.0 mm; depth, 0.8 mm) with upper and lower windows to pass electron beam. Each window is covered with a carbon sealing film (thickness, 15–20 nm) held on a copper grid with nine apertures (diameter, 0.1 mm). The carbon sealing film could bear pressure differences up to one atmosphere. The specimen, placed on the lower carbon film, is kept wet by constantly circulating water vapor (pressure, 60–80 torr; temperature 26–28°C). ATP is applied to the specimen by passing the current through an ATP-containing glass microelectrode. The EC was used in a 200 kV transmission electron microscope (JEM 2000EX; JEOL). The specimen images (magnification, 10,000×) are recorded with the imaging plate (IP) system (PIX system; JEOL). To avoid electron beam damage to the specimen, the total incident electron dose is limited below 5×10^{-4} C/cm^2. Further details have been described elsewhere [5, 6].

A myosin head consists of catalytic activation domain (CAD) and lever arm domain (LD), which are connected with a small converter domain (COD), and the LD is further connected to myosin subfragment-2 extending from the myosin filament backbone (**Figure 3**). Individual myosin heads were position-marked by colloidal gold particles (diameter, 20 nm) via three different antibodies: antibody 1 to the distal region of the CAD [7], antibody 2 to the proximal region of the CAD [7], and antibody 3 to two light chains of the LD [8]. Typical IP images of the bipolar synthetic filaments, with individual myosin heads positon-marked with gold particles, are presented in **Figure 4**. The specimen images could be recorded up to three times under a magnification of 10,000× without giving damage to the
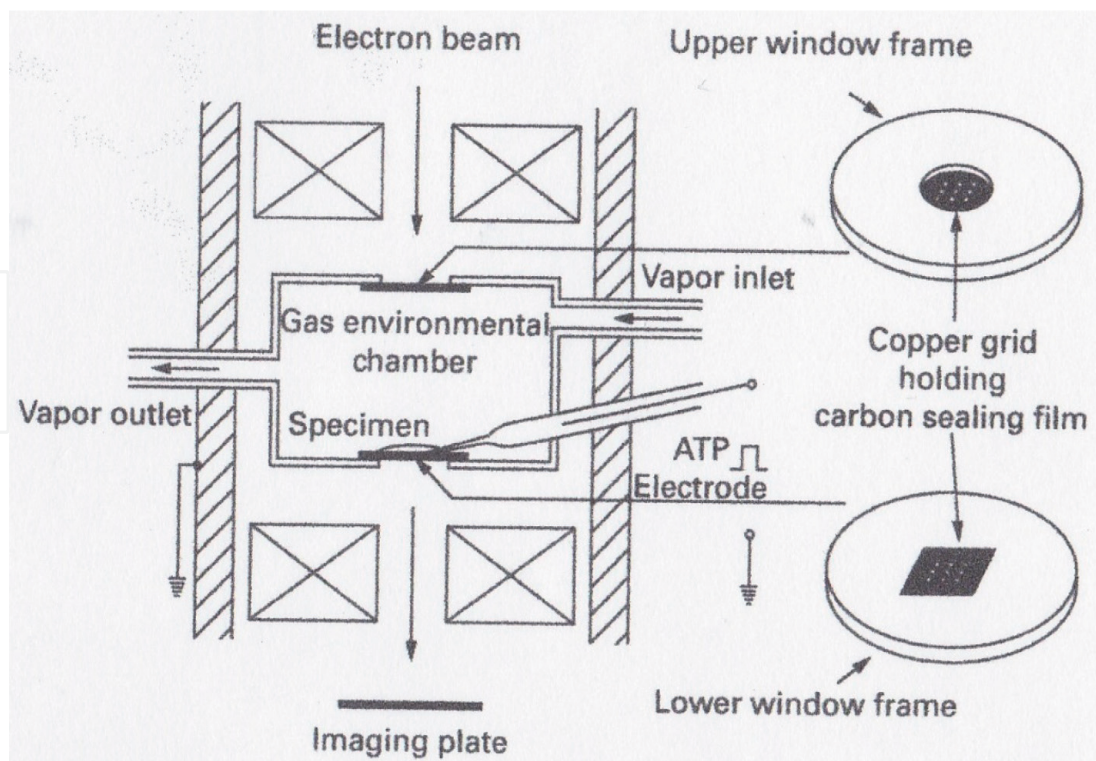

Figure 2.
Diagram showing the EC. The specimen (synthetic myosin filaments) is placed on the lower carbon sealing film and covered with thin layer of experimental solution. ATP is applied to the specimen by passing the current through the ATP-containing glass microelectrode. The specimen images are recorded with the imaging plate. From [6].
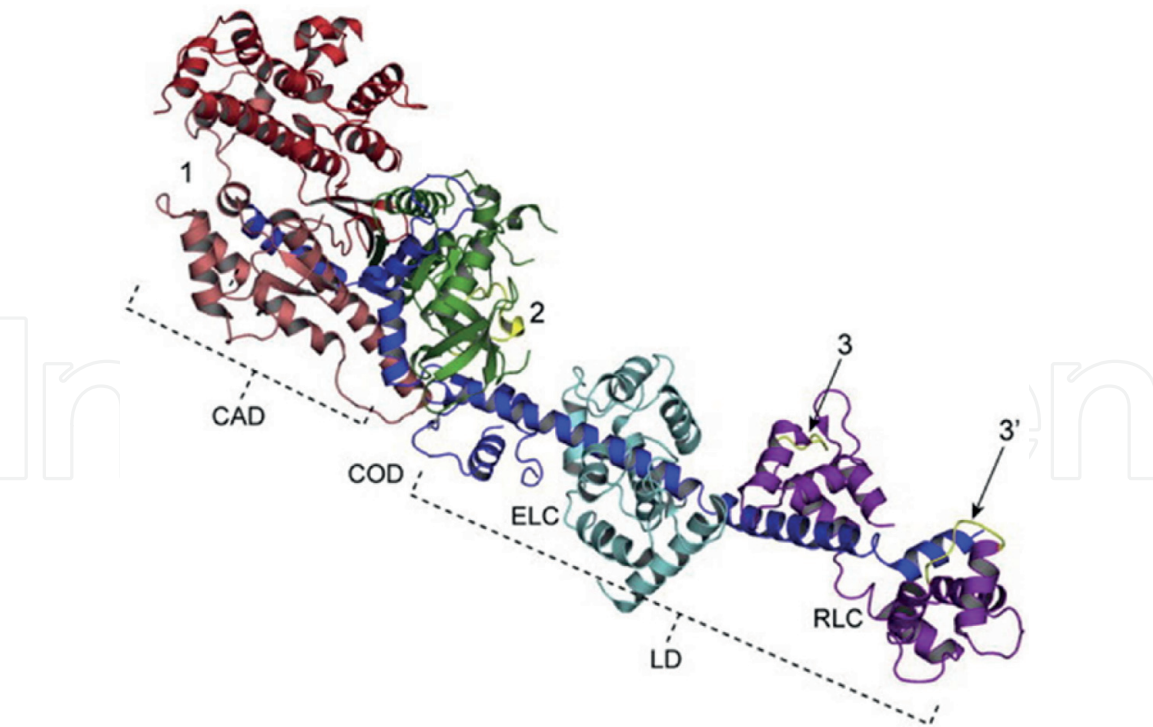
Figure 3.
Structure of a myosin head showing approximate regions of attachment of antibodies 1, 2, and 3, indicated by numbers 1, 2, and 3 and 3', respectively. The catalytic activation domain (CAD) consists of 25 K (green), 50 K (red), and 20 K (dark blue) fragments of myosin heavy chain, while the lever arm domain (LD) is composed of the rest of the 20 K fragment and essential (ELC, light blue) and regulatory (RLC, magenta) light chains. The CAD and LD are connected by the converter domain (COD). Location of peptides around Lys83 and that of two peptides, (Met58-Ala70) and (Leu106-Phe120), are colored yellow. From [9].
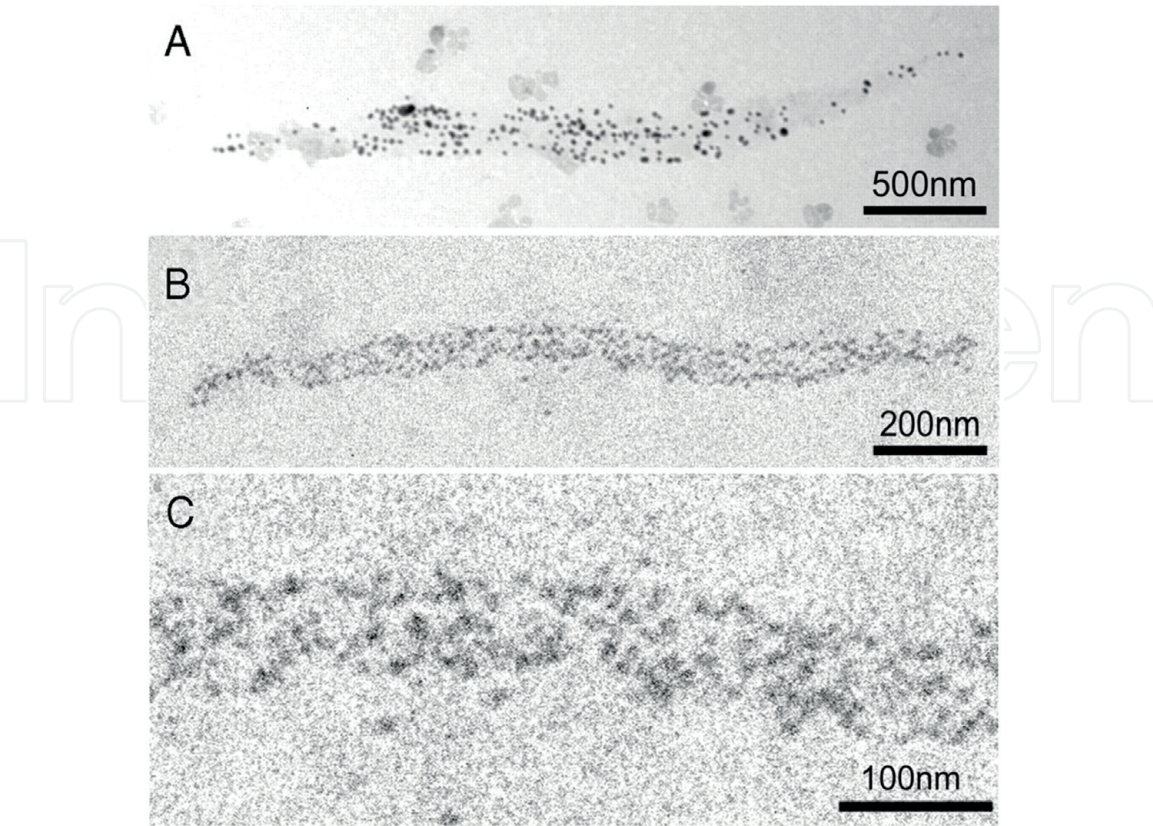

Figure 4.
(A, B) typical IP records of synthetic bipolar myosin filaments with a number of individual myosin heads, position-marked by gold particles. (C) Enlarged IP record showing part of the myosin filament in B. From [7].

specimen (exposure time, 0.1 s). In the above-recording condition, the pixel size was 2.5×2.5 nm, and the average number of electrons reaching each pixel during the exposure time was ~ 10. Reflecting the electron statistics, each gold particle image was composed of 20–50 pixels.

The center of mass position of each gold particle was determined as the coordinates (two significant figures) within a single pixel where the center of mass position was located. These coordinates representing the position of individual myosin heads were compared between two different IP records of the same myosin filaments. The distance D between the two centers of mass positions (with coordinates, X1 and X2 and Y1 and Y2, respectively) was calculated as $D = \sqrt{(X1—X2)^2 + (Y1—Y2)^2}$. Further details of the method of recording have been described elsewhere [5, 6].

3. Stable neutral position of myosin heads in the absence of ATP

Figure 5 shows the results of experiments, in which the image of the same myosin filament was recorded two times at an interval up to several minutes. It was found that the position of individual myosin heads remained almost unchanged
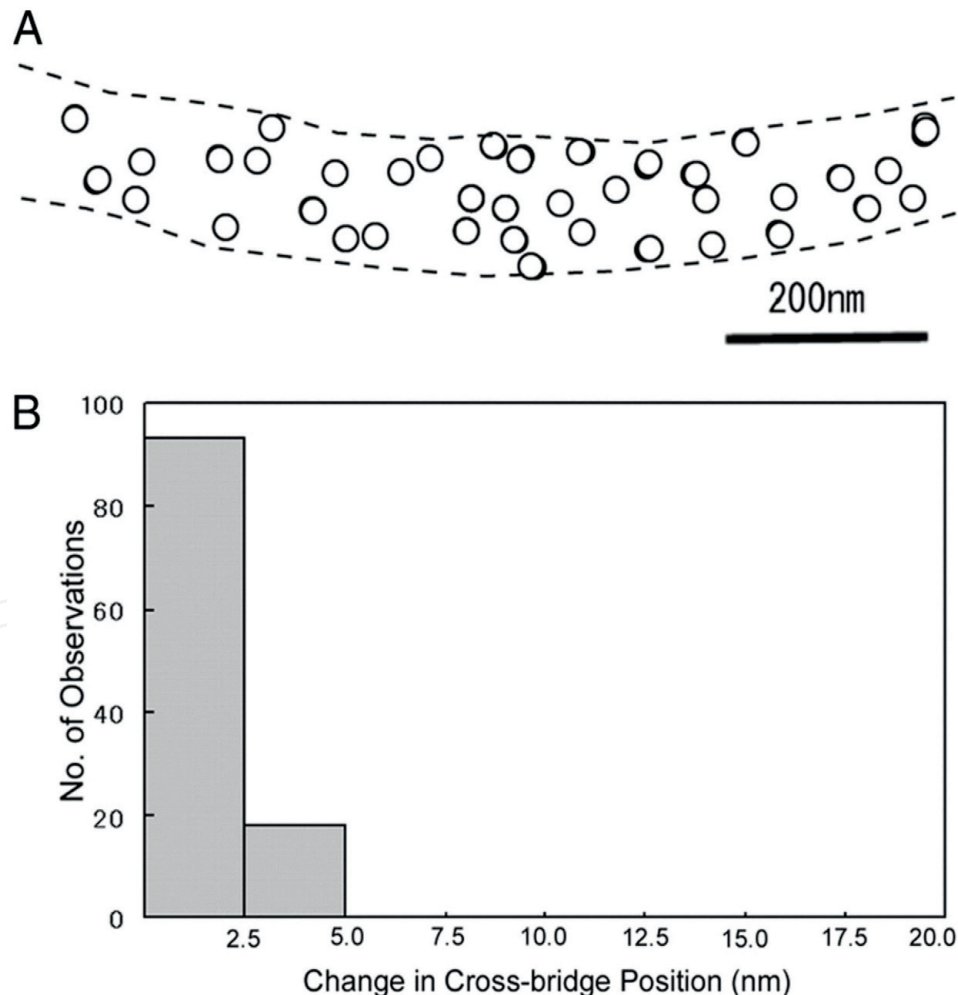

Figure 5.
Stable myosin head neutral position in the absence of ATP. (A) Difference between myosin head positions between two IP records of the same myosin filament on the common coordinates. Open and filled circles (diameter, 20 nm) were drawn around the center of mass position of each gold particle in the first and the second IP records, respectively. Note that filled circles are mostly covered by open circles because of nearly complete overlap between open and filled circles. In this and subsequent figures, broken lines indicate contour of myosin filament. (B) Histogram of distance between the two centers of mass positions of the same gold particle in the first and the second records. From [7].

with time, indicating that the position of each myosin head, time-averaged over 0.1 s (exposure time of the filament image to IP film), remains almost unchanged with time [6]. This result can be taken to indicate that each myosin head undergoes thermal motion around a definite neutral position, thus providing a favorable condition to detect ATP-induced myosin head movement.

4. ATP-induced recovery stroke in the absence of actin filament

On application of ATP to myosin filaments, individual myosin head was found to move in one direction parallel to the filament long axis with the average amplitude of ∼6 nm, as shown in **Figure 6** [7]. If the ATP-induced myosin head
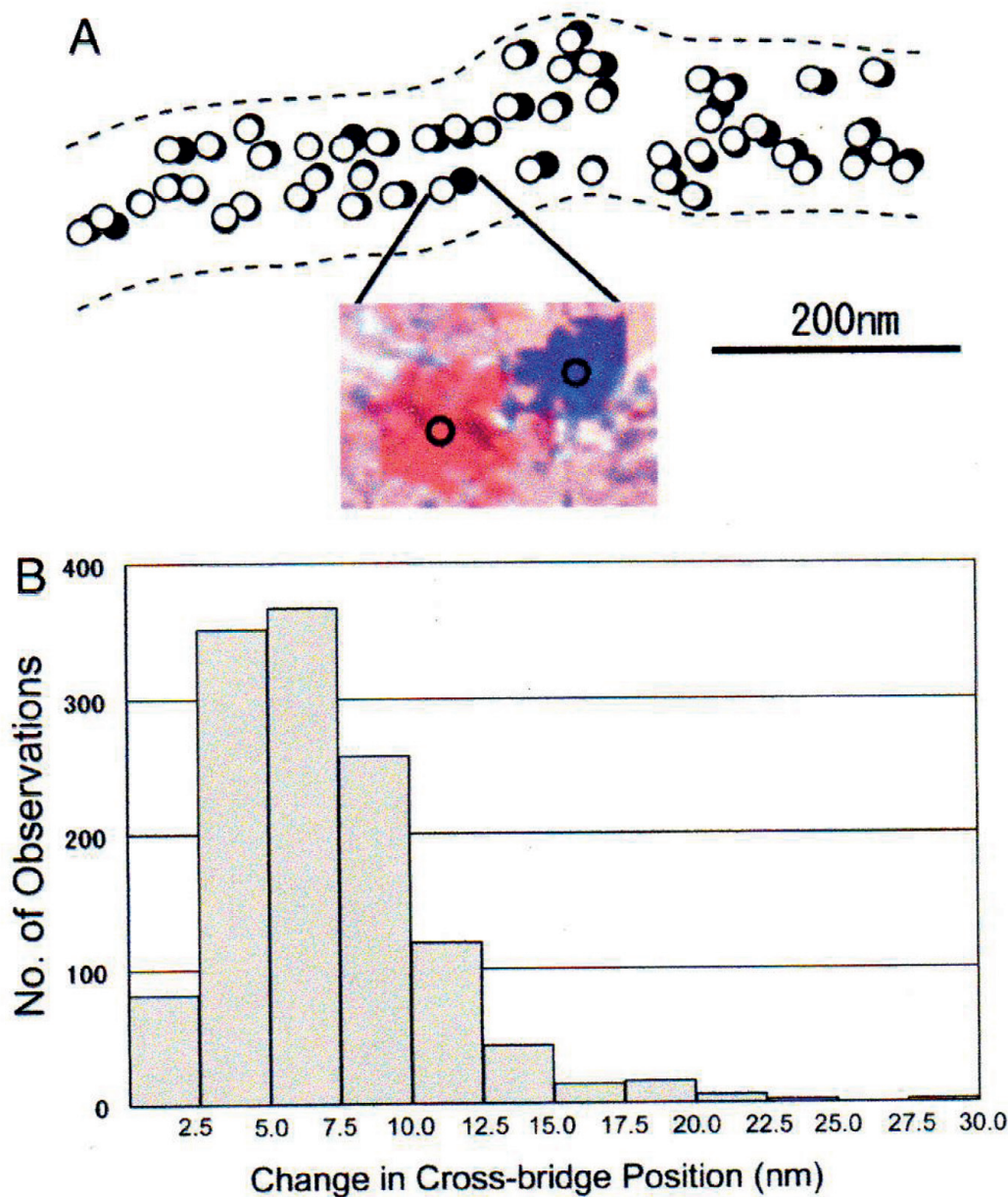

Figure 6.
ATP-induced myosin head movement in the absence of actin filaments. (A) Difference of myosin head position between the two IP records, one taken before, while the other taken after ATP application. Open and filled circles (diameter 20 nm) are drawn around the center of mass position of the same particles before and after ATP applications, respectively. (Inset) An example of superimposed IP records showing the change in position of the same gold particle, which are colored red (before ATP application) and blue (after ATP application). The center of mass position of each particle image is indicated by a small circle in each particle image. (B) Histogram of amplitude distribution of ATP-induced myosin head movement. From [7].
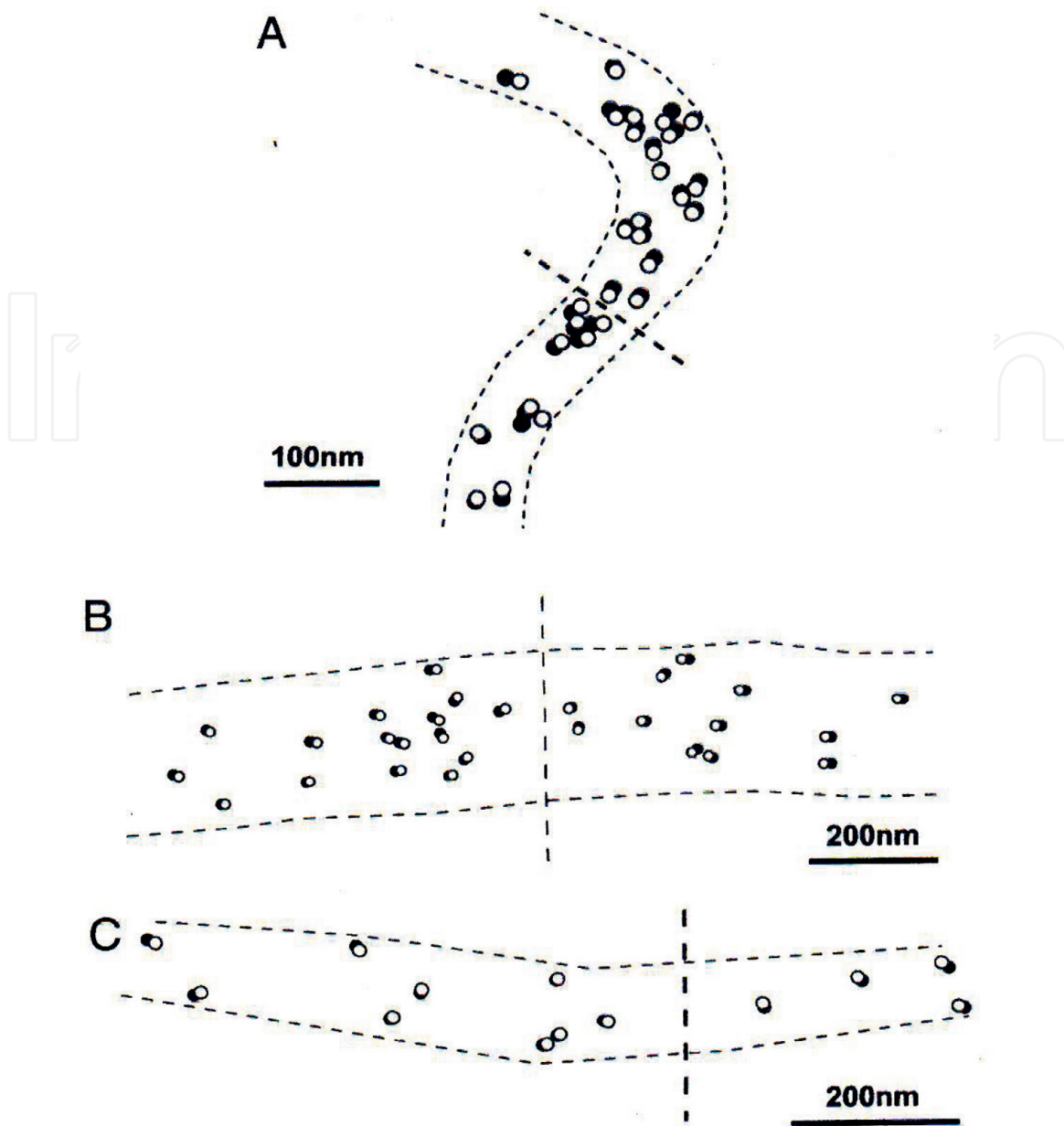
Figure 7.
(A–C) Examples of IP records showing the ATP-induced myosin head movement at both sides of myosin filament bare region, across which myosin head polarity is reversed. Open and filled circles (diameter, 20 nm) are drawn around the center of mass positions of the same particles in the IP records, taken before and after ATP applications, respectively. Note that myosin heads move away from the bare region. Approximate location of the bare region is indicated by broken lines across the center of myosin filament. From [7].

movement was recorded at both sides of the bare region, located at the center of myosin filament, individual myosin heads were found to move away from, but not toward, the bare region, across which the polarity of myosin heads is reversed (**Figure 7**) [7]. These findings indicate that, in the absence of actin filament, individual myosin heads perform a recovery stroke without being guided by actin filaments. In other words, each myosin head can sense the absence (or presence) of actin filaments to decide its direction of movement in response to ATP.

5. Return of myosin heads to the neutral position after exhaustion of ATP

In the absence of actin filaments, we took IP records of the same gold particles three times, i.e., (1) before ATP application, (2) during ATP application, and (3)
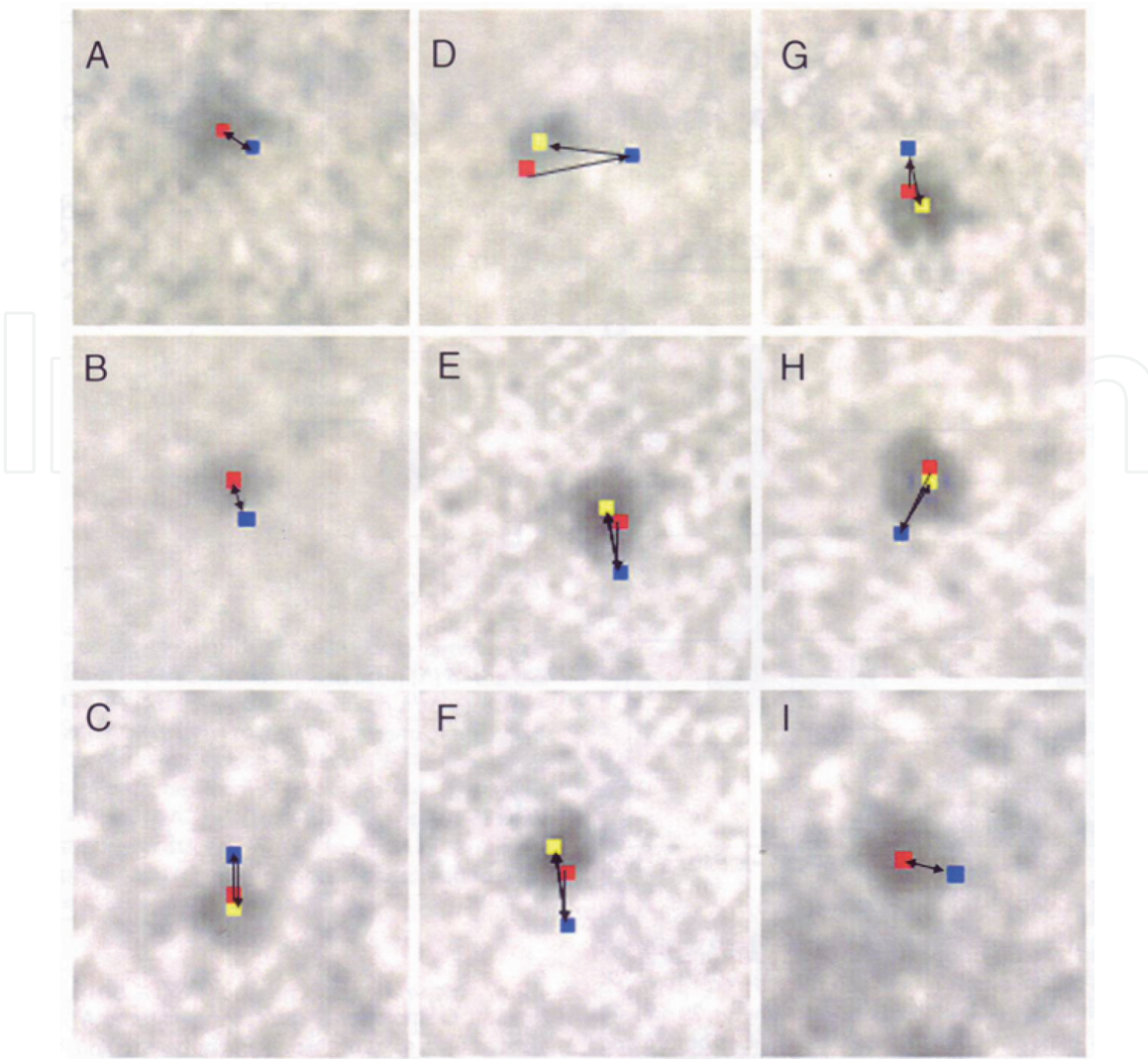
Figure 8.
(A–I) sequential changes in position of nine different pixels (each 2.5 × 2.5 nm), where the center of mass position of corresponding gold particles is located. In each frame, pixel positions before, during, and after complete exhaustion of ATP are indicated by red, blue, and yellow, respectively. Arrows indicate direction of myosin head movement. From [7].

after complete exhaustion of applied ATP (facilitated by adding hexokinase and D-glucose to experimental solution). **Figure 8** shows examples of sequential changes in position of nine different pixels (2.5 × 2.5 nm for each), where the center of mass positions of corresponding particles is located. It was found that myosin heads, which had performed recovery strokes, returned to or toward their initial neutral position after complete exhaustion of ATP. This can be taken to indicate that myosin heads can move in the direction similar to that of power stroke to return to their neutral position [7].

6. Amplitude of recovery stroke at three different regions within a myosin head

Our EC experiments can not only directly record myosin head movement, coupled with ATP hydrolysis but also record myosin head movement at different regions within a single myosin head by using three different antibodies to position-mark myosin heads [8]. As can be seen in the histograms of **Figure 9** A, B, and C, the amplitude of myosin head recovery stroke was the same in the distal region (6.14 ± 0.09 nm, mean ± SEM, n = 1692) and the proximal region (6.14 ± 0.22 nm,
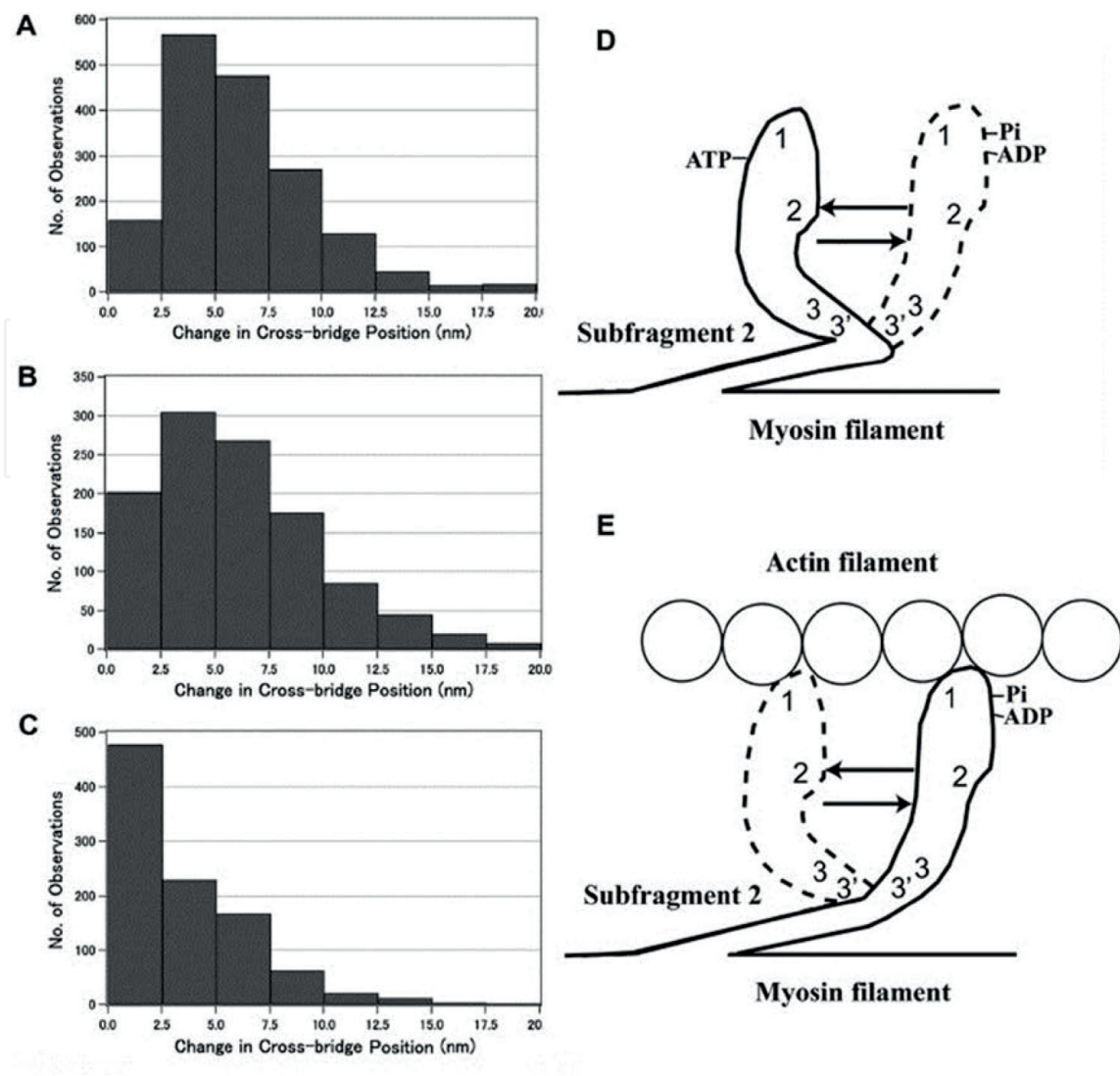
Figure 9.
(A–C) histograms of amplitude distribution of ATP-induced myosin head movement at the distal (A) and the proximal (B) regions of the myosin head CAD, at the two light chains in the proximal region of the myosin head LD. (D, E) Diagrams showing the ATP-induced configuration changes in the absence (D) and the presence (E) of actin filaments, based on the results shown in A–C. From [9].

n = 1112) of myosin head CAD, while it was much smaller at the LD region (3.55 ± 0.11 nm, n = 981) [9]. Based on these results, we can obtain diagrams shown in **Figure 9** D and E, in which myosin head CAD is perpendicular to actin and myosin filaments during the course of recovery stroke and subsequent return to their neutral position [9]. This view is consistent with our published results using the methods of quick-freezing and deep-etch replica that most myosin heads are perpendicular to actin and myosin filaments in relaxed, contracting, and rigor states [10].

7. Two different modes of myosin head power stroke in actin-myosin filament mixture

We also performed experiments, in which ATP-induced myosin head power stroke was recorded using the actin-myosin filament mixture, in which synthetic bipolar myosin filaments were surrounded by a number of actin filaments (**Figure 10**) [11]. Immediately, after mixing the actin and myosin filaments, the filament mixture, myosin heads form tight actin-myosin rigor linkages, some of which may be tension-bearing. Due to finite lifetimes of the rigor linkages [12],
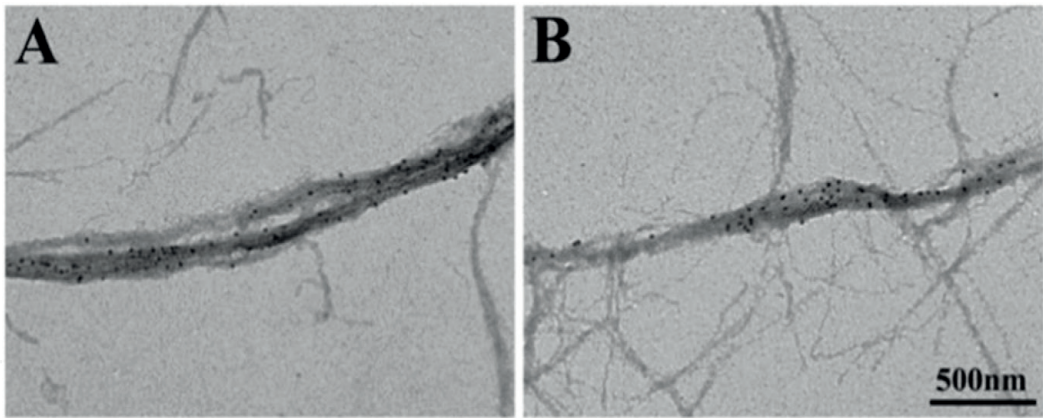
Figure 10.
Conventional electron micrographs of actin-myosin filament mixture. Myosin heads were position-marked with antibody 1 (left) and with antibody 2 (right), respectively. Note that bipolar myosin filaments are surrounded by actin filaments. From [11].
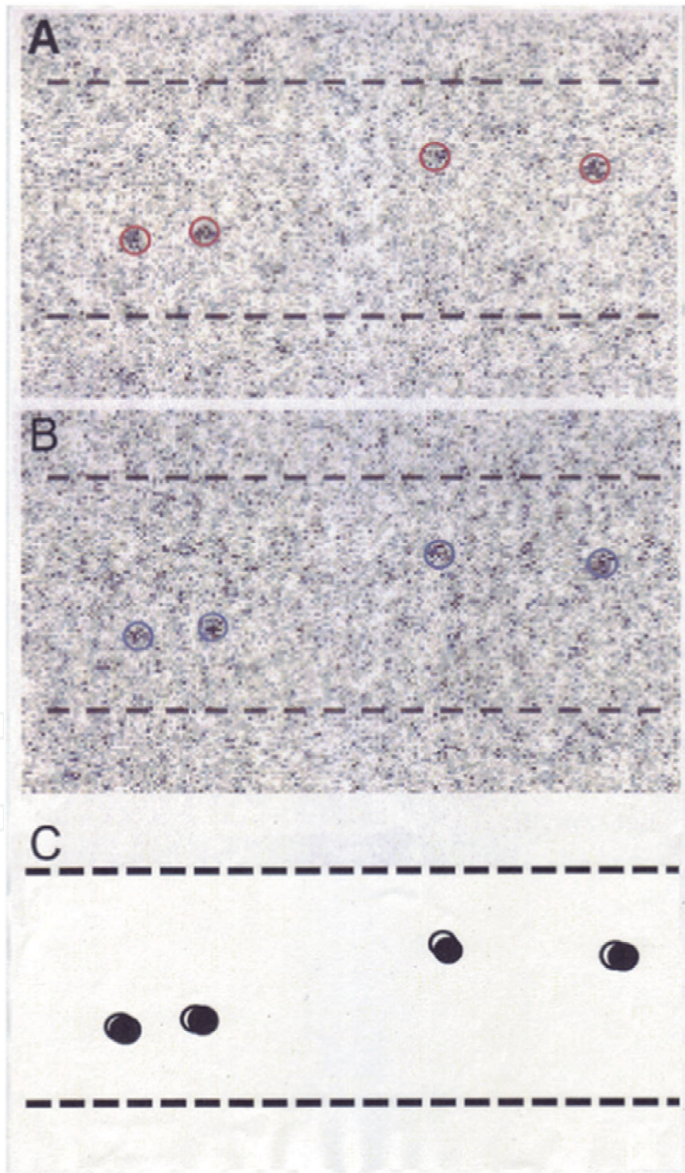

Figure 11.
(A, B) A pair of IP records of the same myosin filament mixture, taken before (A) and after (B) ATP application. Circles (diameter, 20 nm) are drawn around the center of mass position of individual gold particle images, consisting of a number of dark pixels. (C) Diagram showing ATP-induced changes in position of gold particles attached to individual myosin heads with antibody 1. Open and filled circles were drawn around the center of mass positions of the same particle before and after ATP applications, respectively. From [11].
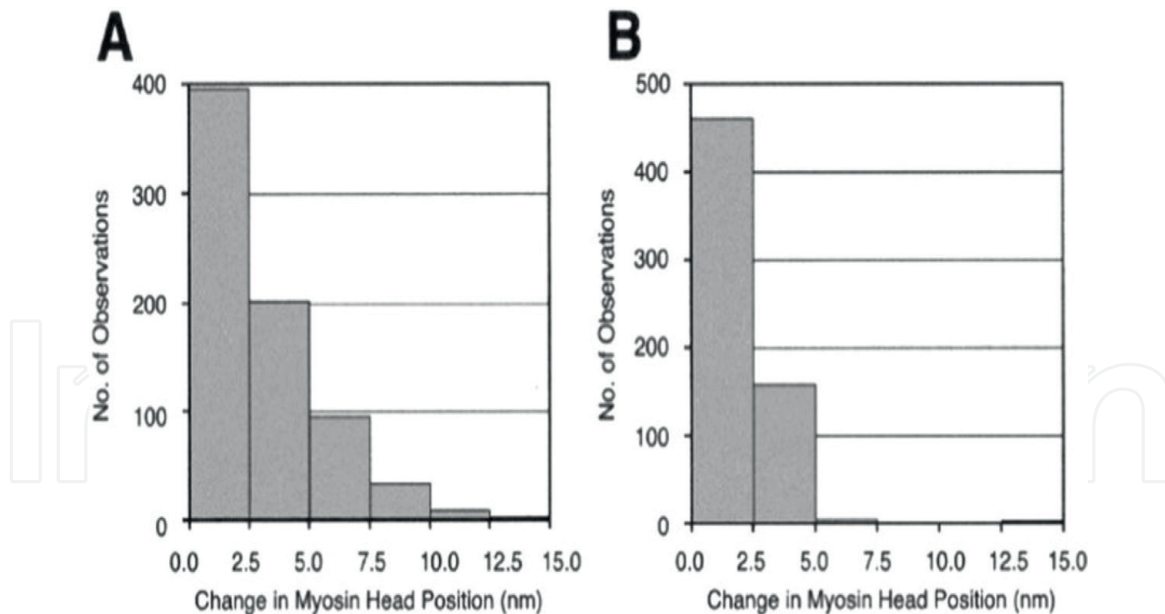
Figure 12.
Histograms of the amplitude distribution of ATP-induced myosin head power stroke at standard ionic strength at the distal (A) and the proximal (B) region of the myosin head CAD. From [11].

such rigor linkages may be broken with time, and myosin heads detached from actin first return to their neutral position and then again form rigor linkages with actin just opposite to them. As a result, all myosin heads are expected to form rigor linkages at their neutral position, where they exert no force, until the beginning of EC experiments at >20 min after the filament mixing.

Since the amount of ATP released from the ATP-containing electrode was limited, the ATP concentration around myosin filaments was estimated to be <10 μM. Reflecting this condition, only a small proportion of myosin heads could be activated by ATP, while the rest of them remained to form rigor linkages. Consequently, the ATP-activated myosin heads may not produce gross filament sliding but may only stretch adjacent elastic structures. **Figure 11** is a typical example of two IP records, taken before and after ATP applications. In accordance with this expectation, the amplitude of ATP-induced myosin head power stroke was small, being 3.3 ± 0.2 nm (mean ± SD, n = 732) at the distal region and 2.5 ± 0.1 nm (n = 613) at the proximal region of the myosin head CAD (**Figure 12**) [10]. If, however, the ionic strength of experimental solution was reduced from 125 to 20 mM, the amplitude of myosin head power stroke increased to 4.4 ± 0.1 nm (mean ± SD, n = 361) at the distal region and 4.3 ± 0.2 nm, n = 305) at the proximal region of the myosin head CAD (**Figure 13**) [10]. The increase in the amplitude of myosin head power stroke by reduction of ionic strength is consistent with our previous report that, at low ionic strength, the magnitude of Ca^{2+}-activated isometric tension in single-skinned fibers increases twofold, while the Mg-ATPase activity remains unchanged, indicating that the force generated by individual myosin heads increases twofold at low ionic strength [13].

Figure 14 shows diagrams showing two different modes of myosin head power stroke depending on experimental conditions. In the standard ionic strength, the amplitude of myosin head power stroke is larger at the distal region than at the proximal region, so that myosin head CAD is oblique to actin filament at the end of power stroke (A). At low ionic strength, the amplitude of myosin head power stroke is the same at both the distal and the proximal regions (B) [10]. This may be taken to imply that, under large loads, the myosin head CAD is oblique to actin filaments at the end of power stroke, while under moderate loads, the myosin head CAD is perpendicular to actin filaments.
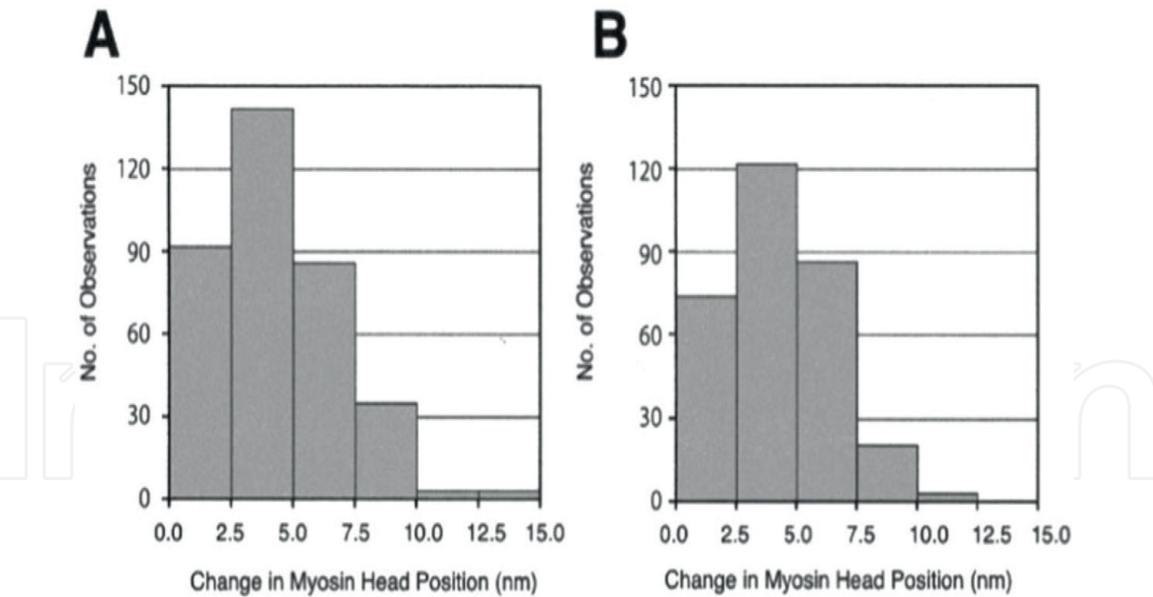
Figure 13.
Histograms of the amplitude distribution of ATP-induced myosin head power stroke at the distal (A) and the proximal (B) region of the myosin head CAD. From [11].
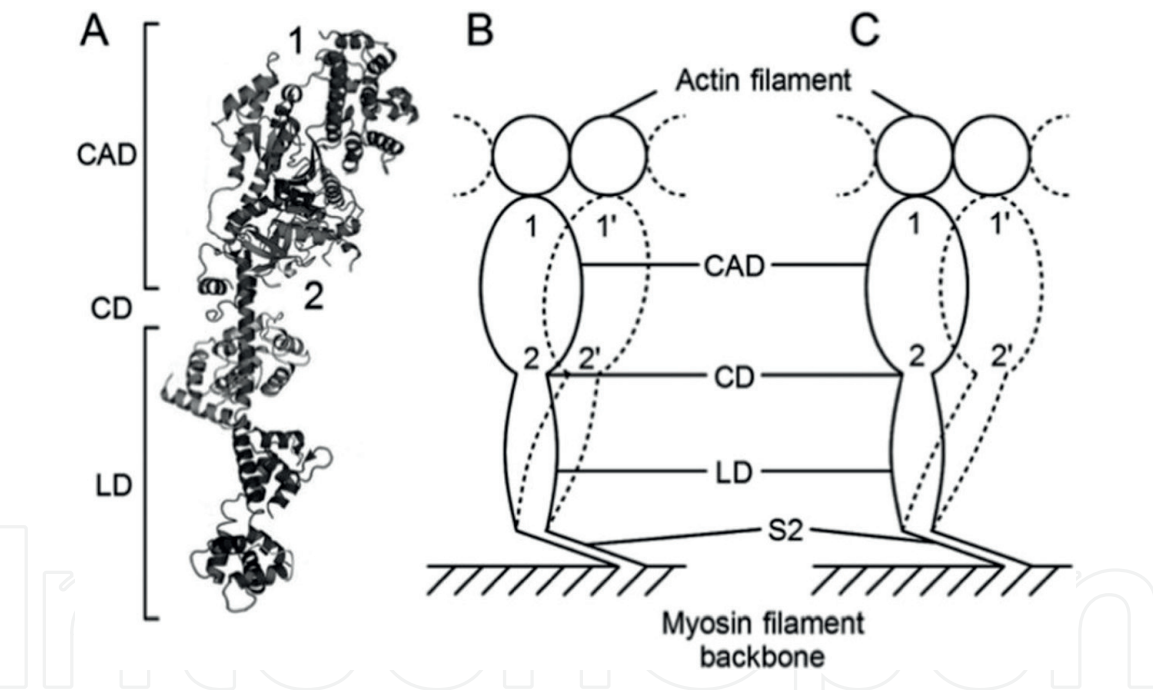

Figure 14.
Diagrams illustrating two different modes of myosin head power stroke, depending on experimental conditions. (A) Diagram of myosin head structure consisting of the CAD, COD, and LD. Approximate attachment regions of antibodies 1 and 2 are indicated by numbers 1 and 2, respectively. (B) The mode of myosin head power stroke at the standard ionic strength. Note that the amplitude of power stroke is larger at the distal region than at the proximal region of myosin head CAD. (C) The mode of myosin head power stroke at low ionic strength. Note that the amplitude of power stroke is the same at both the distal and the proximal regions of the myosin head CAD. From [11].

8. Conclusion

As has been described in this article, the experiments with the EC have the following advantages over any other methods to obtain information about myosin head power and recovery strokes, coupled with ATP hydrolysis: (1) it is possible to visualize and record ATP-induced movement in individual myosin heads within an

electron microscopic field under a high magnification (10,000×); (2) using three different antibodies to myosin head, it is possible to record myosin head movement at three different regions within a myosin head, so that we can obtain information about changes in the mode of myosin head power stroke depending on experimental conditions. The EC experiments can be effectively used to obtain information not only about cardiac and smooth muscle myosins but also about other motile systems such as ciliary and flagellar movements. We hope that the EC experiments will be widely used to open new horizons in the research field of life sciences.

Acknowledgements

Author details

Haruo Sugi[1*], Tsuyosi Akimoto[1] and Shigeru Chaen[2]

1 Department of Physiology, School of Medicine, Teikyo University, Tokyo, Japan

2 Department of Integrated Sciences in Physics and Biology, College of Humanities and Science, Nihon University, Tokyo, Japan

*Address all correspondence to: sugi@kyf.biglobe.ne.jp

IntechOpen

References

[1] Huxley HE, Hanson J. Changes in the cross-striations of muscle during contraction and stretch and their structural interpretation. Nature. 1954;**173**:973-976

[2] Lymn RW, Taylor EW. Mechanism of adenosine triphosphate hydrolysis by actomyosin. Biochemistry. 1971;**16**: 4617-4624

[3] Sugi H, Chaen S, Kobayashi T, Abe T, Kimura K, Saeki Y, et al. Definite differences between in vitro actin-myosin sliding and muscle contraction as revealed using antibodies to myosin head. PLoS One. 2014;**9**:e93272

[4] Fukami A, Adachi K. A new method of preparation of a self-perforated microplastic grid and its applications. Journal of Electron Microscopy. 1965;**14**: 112-118

[5] Suda H, Ishikawa A, Fukam A. Evaluation of the critical electron dose on the contractile ability of hydrated muscle fibers in the film-sealed environmental cell. Journal of Electron Microscopy. 1992;**41**:223-229

[6] Sugi H, Akimoto T, Sutoh K, Chaen S, Oishi N, Suzuki S. Dynamic electron microscopy of ATP-induced myosin head movement in living muscle thick filaments. Proceedings of the National Academy of Sciences of the United States of America. 1997;**94**:4378-4382

[7] Sugi H, Minoda H, Inayoshi Y, Yumoto F, Miyakawa T, Miyauchi Y, et al. Direct demonstration of the cross-bridge recovery stroke in muscle thick filaments in aqueous solution by using the hydration chamber. Proceedings of the National Academy of Sciences of the United States of America. 2008;**45**: 17396-17401

[8] Sutoh K, Tokunaga M, Wakabayashi T. Electron microscopic mapping of myosin head with site-directed antibodies. Journal of Molecular Biology. 1989;**206**:357-363

[9] Minoda H, Okabe T, Inayoshi Y, Miyakawa T, Miyauchi Y, Tanokura M, et al. Electron microscopic evidence for the myosin head lever arm mechanism in hydrated myosin filaments using the gas environmental chamber. Biochemical and Biophysical Research Communications. 2011;**405**:651-656

[10] Suzuki S, Oshimi Y, Sugi H. Freez-fracture studies on the cross-bridge angle distribution at various states and the thin filament stiffness in single skinned frog muscle fibers. Journal of Electron Microscopy. 1993;**42**:107-116

[11] Sugi H, Chaen S, Akimoto T, Minoda H, Minoda H, Miyakawa T, et al. Electron microscopic recording of myosin head power stroke in hydrated myosin filaments. Scientific Reports. 2015;**5**:17500

[12] Nishizaka T, Seo R, Tadakura H, Kinosita K, Ishiwata H. Characterization of single actomyosin rigor bonds: Load dependence of lifetime and mechanical properties. Biophysical Journal. 2000;**79**:962-974

[13] Sugi H, Kobayashi T, Chaen S, Ohnuki Y, Saeki Y, Sugiura S. Enhancement of force generated by individual myosin heads in skinned rabbit psoas muscle fibers at low ionic strength. PLoS One. 2013;**8**:e63658